

## DAMAGE INDEX FOR CROSS SECTION OF RC BEAM-COLUMN MEMBERS SUBJECTED TO MULTI-AXIS LOADING

(Translation from Proceedings of JSCE, No.718/V-57, November 2002)



Satoshi TSUCHIYA



Koichi MAEKAWA

A damage index for the seismic performance evaluation of column members is proposed on the basis of analytical results obtained for multi-axis bending using the fiber technique. The elasto-plastic fracture model for concrete compression makes it possible to calculate a fracture parameter, defined as the reduction ratio in unloading stiffness, for each microscopic cross-sectional area. The average value over the cross section is treated as the index of cross-sectional damage level. It is verified that this proposed index provides an approximation of equivalent damage level up to the yield point after softening of RC beam-column members, not only for one-directional loading but also multi-directional loading. Moreover, this method is also effective for RC members in which the core concrete is confined by stirrups.

**Keywords:** RC beam/column members, damage index, FE nonlinear analysis

---

Satoshi Tsuchiya is a representative director and a second division manager of COMS Engineering Corporation, Japan. He obtained his D. Eng. from the University of Tokyo in 2001. He has been trying to make high-grade nonlinear structural analysis fit for practical use. His research interests cover the seismic performance evaluation and numerical simulation of reinforced concrete structures.

---

Koichi Maekawa is a professor in the Department of Civil Engineering at the University of Tokyo, Japan. He earned his D. Eng. from the University of Tokyo in 1985. The structural mechanics and constitutive laws for reinforced concrete have been investigated as his academic major background. He joined the project for development of self-compacting concrete in 1985-1989. After innovation of its prototype, he has been engaged in the project for micro-structural development of cementitious materials and computational durability assessment.

## **1. INTRODUCTION**

Dynamic nonlinear analysis using mechanical materials models not only makes it possible to obtain displacement response values or cross-sectional forces for a structure, but also the stress or strain (maximum experienced value) at each location. Such information is of great value in developing quantitative evaluations of the degree of material damage, and is difficult to obtain through nonlinear analysis based on mechanical member models. Essentially, it makes detailed seismic performance evaluations possible on the basis of stress or strain history. For example, in applying three-dimensional nonlinear analysis to the seismic performance-based design of underground LNG tanks [1], the limit state of seismic performance Level 2 might be the point at which the maximum value of principle compressive strain reaches twice the strain corresponding to uni-axial compressive strength. If the response exceeds this limit, permanent damage arises in concrete elements resisting the in-plane shear force [2], and the structure will require restoration after an earthquake.

The response strain of component materials can be also obtained for RC beam-column members, but use of the maximum strain to judge the limit state of a structure such as an LNG tank, the following problems arise:

1) The strain gradient is very large in the case of beam-column members (as compared with shell structures), and the maximum strain is concentrated in a region of quite small volume. This does not always correspond to the damage incurred at the member level. On the other hand, in the case of shell structures, because the strain gradient is low and damage is distributed over a wide area, the maximum strain among all component elements approximately represents the overall damage to the structure.

2) In the case of beam-column members, local strain values tend to be affected by the details of mesh definition, whereas member displacement is the integrated value of strain. In particular, the influence of mesh definition over the cross section is large, while it is also significant in the axial direction in the post-peak range after maximum capacity. On the other hand, in the case of shell structures, the local strain value is affected little by the mesh definition because the strain gradient is small.

The response displacement at the column top, whose dimension is integrated value of strain, has been used as an evaluation index of damage at the member level for RC column members [3]. It can be said this method of judgment is ideal, given the above background.

However, where RC beam-column members exhibit a complex response due to two-axis bending, and where axial force vary significantly in the compression-tension range, direct application of the limit state of displacement based on monotonic loading in an experiment would be too hasty a step. Even if loading and response are limited in one direction, the degree of damage cannot be estimated only from the maximum response displacement, since damage incurred during reversed cyclic loading and under monotonic loading is different. Moreover, in the case of structures consisting of multiple beam-column members, such as Rahmen-type structures with intermediate beams, it is inconvenient to calculate the response displacement of each member during an earthquake.

In this study, a new evaluation index is investigated against this background; the new index is equivalent to the limit state under conventional member displacement, but its applicability is extended to three dimensions. By making use of an index that links mechanical damage level with universal material constitutive models in evaluating loading conditions and confinement effect, etc., it is aimed to establish an evaluation criterion for the limit state depending on the degree of damage. Here, the target is a damage state in which the maximum capacity of flexure-prone RC column members is exceeded and loading degrades to approximately the yield load. Generally, this damage situation is linked to the Level 2 limit state of seismic performance (defined as “no collapse, possible reuse after earthquake without strengthening”) for structures consisting of beam-column members [3].

## **2. FRACTURE PARAMETER OF CONCRETE AND CROSS-SECTIONAL DAMAGE INDEX**

### **2.1 Analytical Model**

The fiber technique is chosen for three-dimensional analysis in this study. The stress field along the member

axis is assumed to be uni-axial and the Euler-Kirchoff hypothesis is adopted; that is, strain is proportional to distance from the neutral axis. The member cross section is divided into microscopic cells. Material mechanical models are applied to the concrete and reinforcing bars constituting each microscopic cell [4]. In this study, the elasto-plastic fracture model [5] is used for concrete and Kato's model [6] for the cyclic behavior of reinforcement.

While the full material constitutive model for concrete consists of compression, tension, crack plane re-contact mechanics, and historic damping, as shown in Fig. 1 (a), it has been confirmed that deviations in response value are limited to several percent even if the simplified model shown in Fig. 1 (b) is used. For the relationship between average stress and average strain of the main reinforcing bars after buckling, the model by Dhakal et al. [7] (derived from Pinto et al.'s model [8]) is employed. As explained in detail in Section 5, the simulation considers the averaged confinement effect of lateral ties over the cross section, as in the previous study.

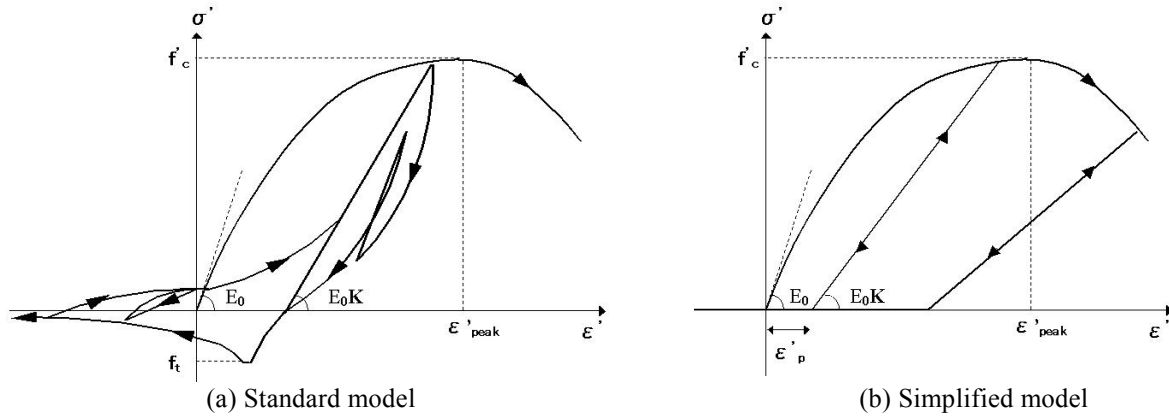


Fig. 1 Material models and fracture parameter of concrete

Summary explanations of these analytical and material models, as well as their applicability, are discussed in the references, for example [4][8][9]. Variations in shear deformation resulting from varying amounts of lateral ties are not considered. However, variations in response flexural behavior according to the arrangement method of lateral ties are indirectly taken into account in the material models by considering the buckling behavior of main reinforcing bars and the confinement effect of the core concrete. If post-peak behavior is to be the target, it is necessary to take into consideration compression softening and the confinement effect of concrete, spalling of cover concrete, and buckling of the main reinforcing bars. Generally, neglect these characteristics in analysis results in evaluations that fall on the dangerous side for member deformation, while confinement effect evaluations are safe.

So as to clarify the relationship between member deformation and degree of cross sectional damage, the effect of pull-out of the main reinforcing bars from the footing is neglected in the analysis.

## 2.2 Cross Section Damage Index

From among the several types of response value available for analysis when using the fiber technique, the authors focus in this study on the fracture parameter of concrete, which is calculated for each microscopic cell. In the elasto-plastic fracture model scheme, the fracture parameter is strictly defined as the reduction (as a ratio) in unloading stiffness under full three-dimensional stress and strain fields. Physically, it means the volume ratio in which the shear elastic strain energy is stored [10]. This parameter is unity in the initial non-damaged state, and can potentially reach zero at complete shear collapse of the material. The idea is to apply this as an index of concrete damage level in seismic performance evaluations. The elasto-plastic fracture model and fracture parameter for normal-strength concrete, as formulated for full three-dimensional stress and strain fields, can be simply reduced to uni-axial states as Eq. (1) to Eq. (3) [5].

$$\sigma' = E_0 K \{ \varepsilon' - \varepsilon'_p \} \quad (1)$$

$$K = \exp[-0.73 \varepsilon'_{\max} \{ 1 - \exp(-1.25 \varepsilon'_{\max}) \}] \quad (2)$$

$$\varepsilon'_p = \varepsilon'_{\max} - 20\{1 - \exp(-0.35\varepsilon'_{\max})\} / 7 \quad (3)$$

where,  $K$  is the fracture parameter,  $\varepsilon'$  is normalized axial strain divided by  $\varepsilon'_{peak}$  (i.e. the strain corresponding to compressive strength),  $\varepsilon'_p$  is normalized plastic strain divided by  $\varepsilon'_{peak}$ ,  $\varepsilon'_{\max}$  is the maximum experienced value of normalized strain,  $\sigma'$  is the normalized compressive stress divided by uni-axial compressive strength, and  $E_0$  is a constant value reflecting initial stiffness (= 2.0).

Considering points 1) and 2) in Section 1, the authors choose to investigate the sectional averaged value of the fracture parameter  $K(x, y)$  within a referential section. Because it is useful to set the parameter to zero at the initial stage and to unity upon complete material failure in a performance evaluation,  $\{1 - K(x, y)\}$  is chosen as the indicator of local mechanical damage. Its sectional averaged value within a referential section is determined as the cross-sectional damage index  $\bar{F}$ , as given by Eq. (4).

$$\bar{F} = 1 - \bar{K} \equiv \frac{1}{A_c} \int_{A_c} (1 - K) dA \approx 1 - \frac{\sum K \cdot \Delta A}{A_c} \quad (4)$$

where,  $\bar{F}$  is the cross-sectional damage index,  $\bar{K}$  is the average fracture parameter,  $K$  is the local fracture parameter for each microscopic cell, and  $A_c$  is the concrete cross-sectional area.

This aim is to check the damage index for each member cross section, and to determine the limit state by selecting its maximum value. This damage index represents material information over a certain length in the member axial direction. The relationship between the distribution of fracture parameter over the cross section and the damage index is illustrated roughly in Fig. 2.

Physically, the damage index represents the normalized degradation of absorbed elastic strain energy for the concrete [5]. Therefore, plasticity does not play a role in the index. Plastic deformation represents slip in the material's physical organization while the stiffness is retained. In the case of repair or retrofitting after seismic action, it is desirable to use more direct information related to local damage. Consequently, such an index that does not include plastic deformation is thought to be most suitable. The influence of compressive plasticity is reflected as member displacement, such as subsidence of the column top, and plasticity within the cross section is taken into account through the response displacement of a structure or member.

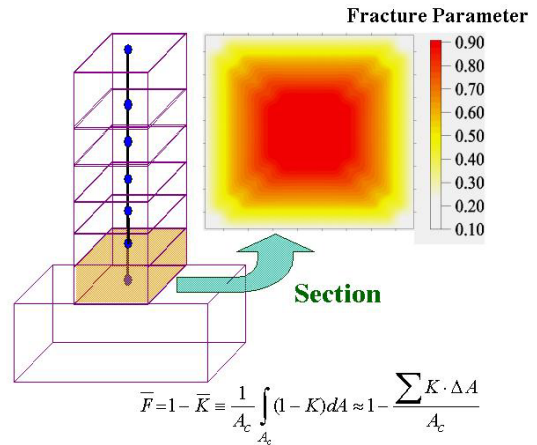


Fig. 2 Space averaging of local fracture

### 3. RELATIONSHIP BETWEEN MEMBER DISPLACEMENT UNDER ONE-AXIS LOADING AND DAMAGE INDEX

Figures 3.1 to 3.3 present analytical results for RC columns with dimensions representative of piers used for road and railway bridges in Japan under static reversed cyclic loading. In these diagrams, the cross-sectional damage index  $\bar{F}$  of the element corresponding to the maximum moment cross section and the yield load (the load at which the reinforcing bar at the center of gravity of the tension force begins to yield [3]) are also shown. The points at which the damage index reaches at 0.385 (= 0.500/1.3), 0.417 (= 0.500/1.2), and 0.500 are indicated, respectively. The reason for choosing values that are divided by 1.3 and 1.2 is that this adds a safety margin to the response value, and so will give helpful information for defining an appropriate safety factor. The dimensions of the target columns illustrated in Figs. 4.1 to 4.3 were determined in consideration of reference literature [11][12][13]. The average axial compressive stress is approximately 1.0 [N/mm<sup>2</sup>]. Figure 3.1 also shows the analytical results under monotonic loading to allow comparative study. Here, the reason for the softening phenomenon in the load-displacement diagram is that concrete at the compressive edge reaches the strain softening range, and the neutral axis over the cross section shifts toward the center because buckling of the reinforcing bars is considered.

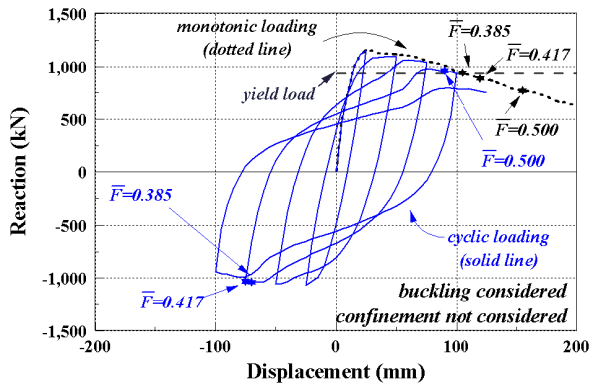


Fig.3.1 Uni-axis cyclic response of railway-type column

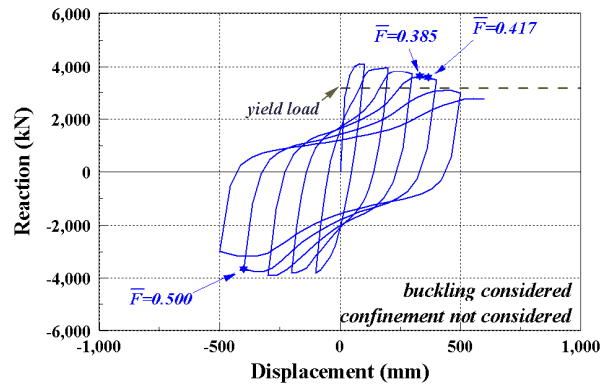


Fig.3.2 Uni-axis cyclic response of road-type column

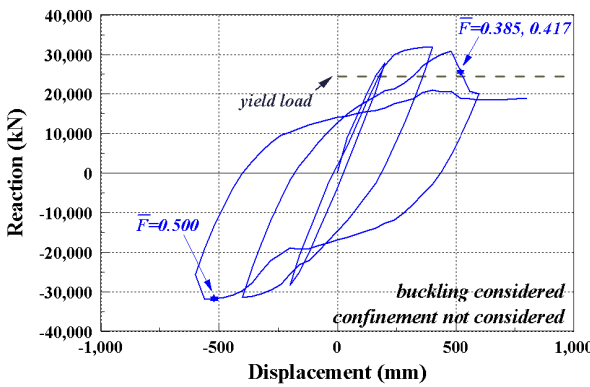


Fig.3.3 Uni-axis cyclic response of hollow column

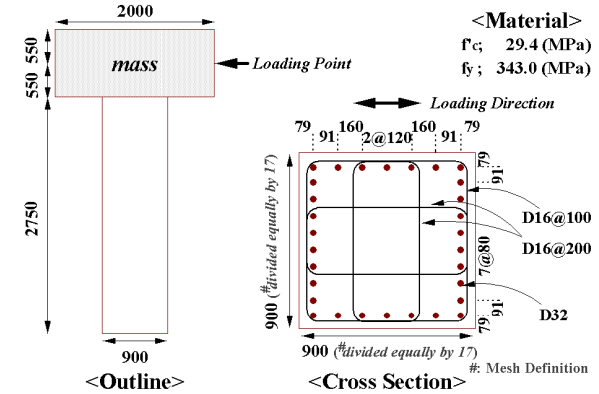


Fig.4.1 Structural dimensions of railway type-column [11]

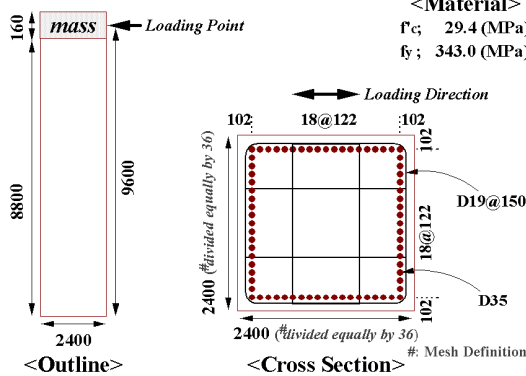


Fig.4.2 Structural dimensions of road type-column [12]

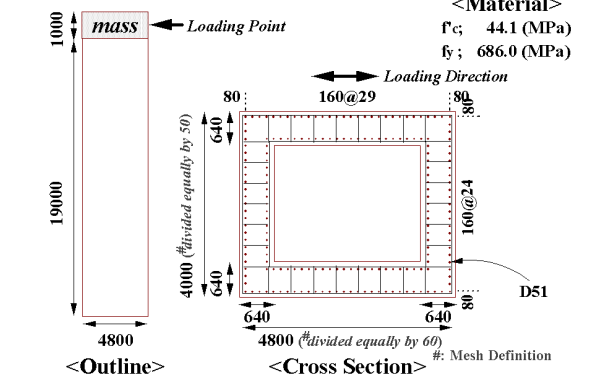


Fig.4.3 Structural dimensions of hollow column [13]

As for the mesh definition, the element length in the region of maximum moment is set to 200 [mm]. The relationship between concrete stress and strain [5] is specified in terms of a 200 [mm] experimental test piece, and the region of concentrated compressive deformation in the softening range is close to the size of the cylindrical compressive test piece, 200 [mm] [14][15]; consequently, this length is chosen as the mesh size. It was demonstrated in advance that the restoring force characteristic is barely affected until the softening behavior becomes significant when the element length is changed from 100 to 300 [mm]. The influence of these variations in element length on response value  $\bar{F}$  at the maximum moment cross section is about 15 [%] at most. The mesh division over the cross section is illustrated in Figs. 4.1 to 4.3.

The analytical results show that the response displacement point at which the horizontal load decreases from the peak capacity somewhat is approximately coincides with the cross-sectional damage index  $\bar{F} = 0.500$  ( $\therefore \bar{K} = 0.500$ ) for the three columns. It is confirmed that the average fracture parameter  $\bar{K}$  suddenly decreases from about 0.600 after the point of maximum capacity. Displacement values when the damage index reaches 0.500 are different in reversed cyclic and monotonic loading, and the proposed index is able to

reflect the different damage situation according to the loading path, as shown in **Fig. 3.1**. The damage index does not change very much along the unloading and reloading path, and it is significantly higher along the virgin loading path. This means that the ability to possess the elastic strain energy of concrete constituting cross section does not decrease when the previous loading path is selected again.

In **Fig. 5**, the relationship between response displacement and damage index is investigated as the weight of the superstructure only is varied by up to four times for the column shown in **Fig. 4.1**. Ductility in the horizontal direction decreases when the axial force is high. In such a situation, it is found that the response displacement point at which the horizontal load decreases from the peak capacity somewhat approximately coincides with the cross-sectional damage index  $\bar{F} = 0.500$ . The damage index calculated from the average fracture parameter approximately corresponds to the ultimate displacement that sustains the yield load, and it changes with axial force. In the case of a high axial force, the influence of core concrete confinement effect on the response is high; however, the analysis shown in **Fig. 5** does not take into account the confinement effect, so it may underestimate ductility somewhat. The applicability of the damage index to confinement effect is investigated later.

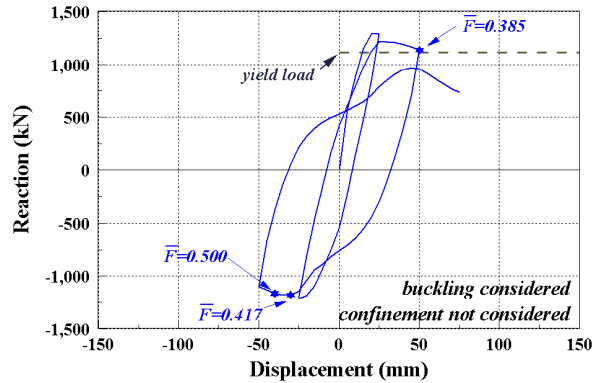


**Fig. 5** Effect of high axial compression on ductility

Because the initiation of spalling of the cover concrete is not sufficiently clear in the analytical model used in this study, predictive accuracy may decrease somewhat when an RC column without axial force is the target. However, the influence is comparatively small under conditions where axial force is acting, so this may be treated as a minor concern for the purposes of this study.

#### **4. APPLICABILITY OF DAMAGE INDEX TO MULTI-AXIS LOADING**

Mechanical universality for arbitrary loading paths on multiple axes is one of desired characteristics of the proposed damage index, and the universality is different point from the current method in which the limit state is defined by response displacement. For the column indicated in **Fig. 4.1**, simulations in which horizontal diagonal loading is applied along the 45 and 22.5 degree axes are carried out in order to investigate the relationship between response displacement and damage index. The analytical results are presented in **Figs. 6.1** and **6.2**.

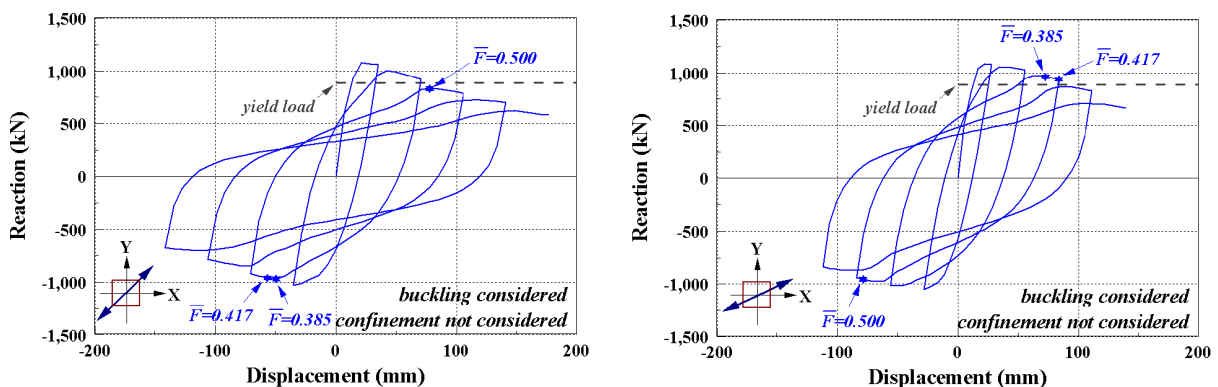


**Fig.6.1** Restoring force under skew loading (45 degree) **Fig.6.2** Restoring force under skew loading (22.5 degree)

For both loading directions, it can be said that the point at which the damage index is 0.500 corresponds to the situation where the yield load is maintained in the softening range after peak capacity. The maximum strain is introduced at the corner of the member cross section when diagonal loading is applied; besides, the

value of maximum strain is much larger than that at the other part. Consequently, choosing the maximum strain as an index for the limit state makes the performance evaluation of members difficult. Even if a very large strain is introduced and significant local damage occurs at a corner, its influence on cross section damage is low as long as the damaged area is small compared to the overall cross-sectional area. In other words, it is not appropriate to judge seismic performance Level 2 using only the maximum compressive strain. Incidentally, the reason that the maximum capacity is almost the same for different loading axes is that the amounts of main reinforcement in the two directions orthogonal to the cross section are different.

**Figure 8** shows the analytical results for a case where an artificial seismic waveform was applied in three orthogonal directions, as shown in **Fig. 7**, for the column in **Fig. 4.1**. Bending compression occurs on all four sides, and concrete damage is also distributed on all sides. In this case, it is generally difficult to apply the limit displacement identified in advance from response behavior in only one direction. In fact, while the limit displacement identified from reversed cyclic static loading in one direction (that is, the displacement with the damage index as 0.500) is 900 [mm] as indicated in **Fig. 3.1**, the damage index reaches 0.500 under multi-axis dynamic loading when displacement in the X-direction is 45.5 [mm] and in the Y-direction is 43.0 [mm].

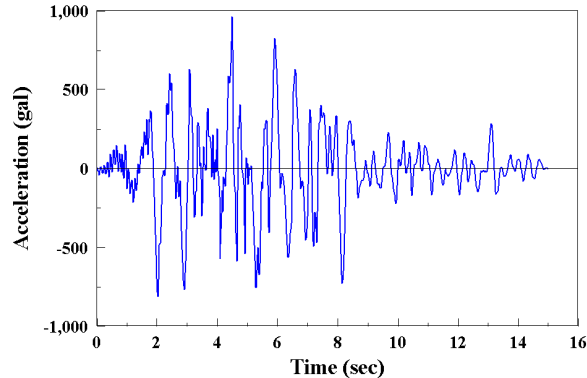


**Fig.7.1** Three-axis input motion (X-direction)

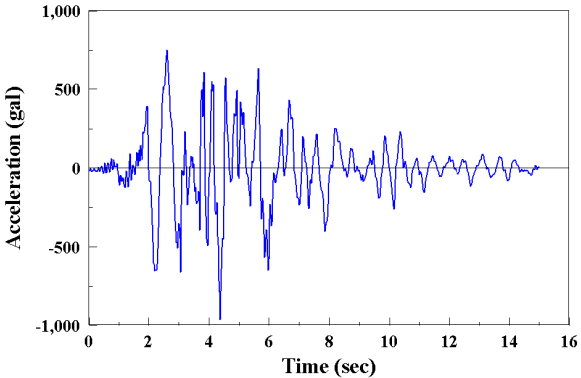


**Fig.7.2** Three-axis input motion (Y-direction)

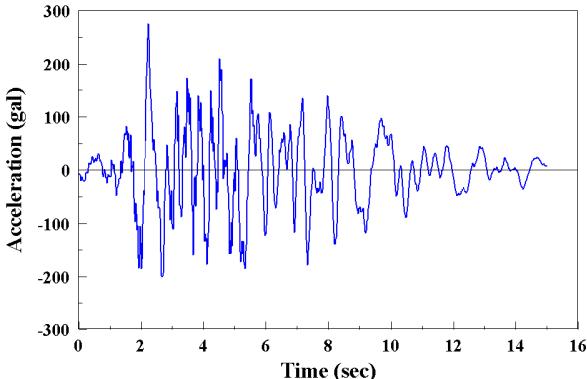


**Fig.7.3** Three-axis input motion (Z-direction)

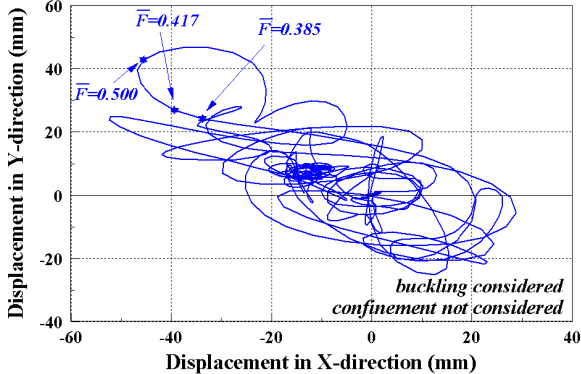


**Fig.8** Dynamic response analysis under multi-axis seismic motion

**5. APPLICABILITY OF DAMAGE INDEX TO CONFINEMENT EFFECT BY LATERAL TIES**

The relationship between core concrete stress and strain along the member axial direction is affected by the arrangement of lateral ties. Generally, concrete ductility is improved and a strength gain is achieved by increasing confinement. Core concrete with improved ductility inherently means that member ductility is superior. This behavior can be estimated using full three-dimensional nonlinear analysis based on three-dimensional material constitutive models [16][17]. And it is possible to express this effect indirectly in simulations based on the fiber technique by changing the relationship between concrete stress and strain along the member axis for each location according to the arrangement and quantity of lateral ties in the transverse direction.

According to previous experimental research on three-dimensional constitutive models, confinement effect can be rationally characterized by applying an evolution law to fracturing, as shown in **Fig. 9** [17]. Namely, the apparent strength gain and ductility improvement arising from the confinement effect derives from restrained fracturing, whereas the evolution of plastic deformation is not affected by confinement effect at all. Then the confinement effect is formulated by changing the fracture evolution rule used in the relationship between uni-axial stress and strain. By means of this analytical approach, the ductility improvement of column members resulting from confinement and the rationality of the cross-sectional damage index are investigated.

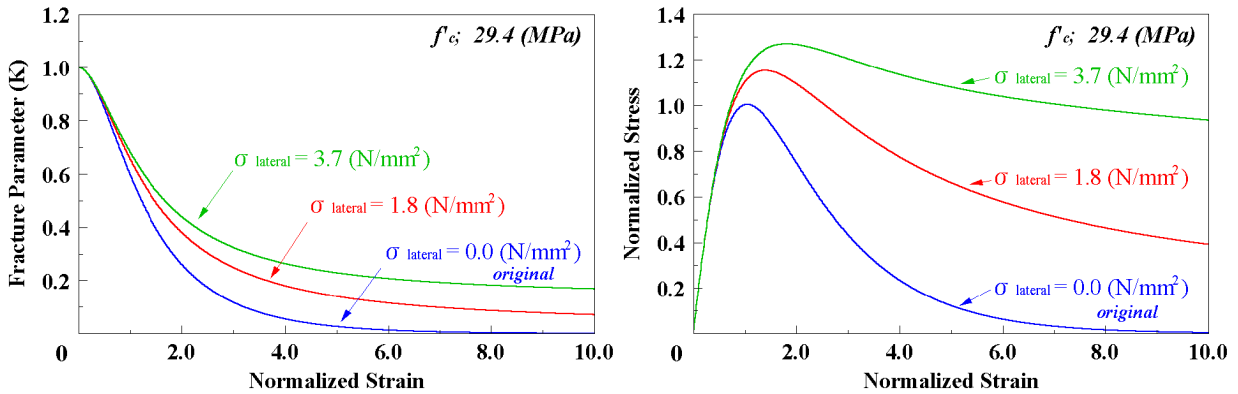


**Fig.9** Lateral confinement of concrete and delayed fracturing [16][17]

The relationship between load and displacement at the top of the column, and the corresponding damage index, are indicated in **Figs. 10.1 to 10.5**, where the confinement effect of the core concrete varies uniformly over the cross section. In order to clarify the influence of confinement, the RC columns shown in **Fig. 4.1** and **4.2** are selected as the target. The dotted lines in **Figs. 10.1 to 10.5** represent analytical results without the confinement effect; these are the same as the results in **Figs. 3, 5, and 6**. Here, changes in the fracture evolution law are expressed as shown in **Fig. 9**, referring to research by Irawan and Pallewatta et al. [16][17]. Their work dealt with compressive loading along the centerline axis, and this loading condition is different from that in our investigation, where flexure is prominent. In the case that anchorage of the lateral ties is sufficient and that all bars reach the yield point in the highly plastic region, however, it is also examined that the hypothesis in **Fig. 9** may be considered close to the confinement effect of concrete under bending compression. A uniform transverse confinement stress is defined according to the assumed arrangement and the strength of the lateral ties in this study: 3.7 N/mm<sup>2</sup> for the medium-scale column shown in **Fig. 4.1** and 1.8 N/mm<sup>2</sup> for the large-scale column shown in **Fig. 4.2**, respectively.

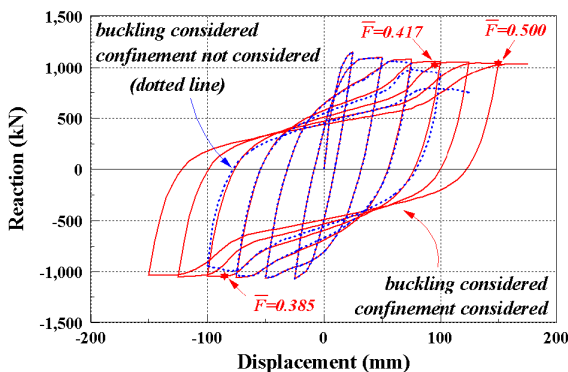


**Fig.10.1** Confinement effect on response and damage index of medium-scale section

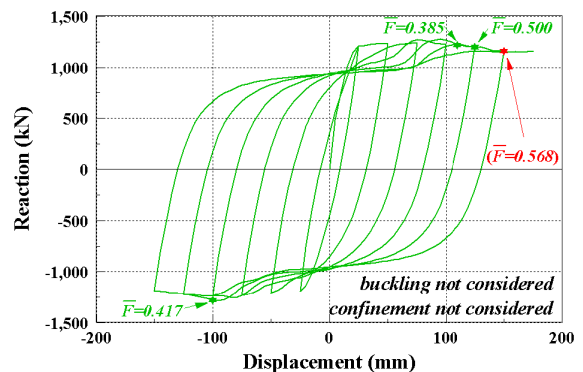


**Fig.11.1** Buckling effect on response and damage index of medium-scale section

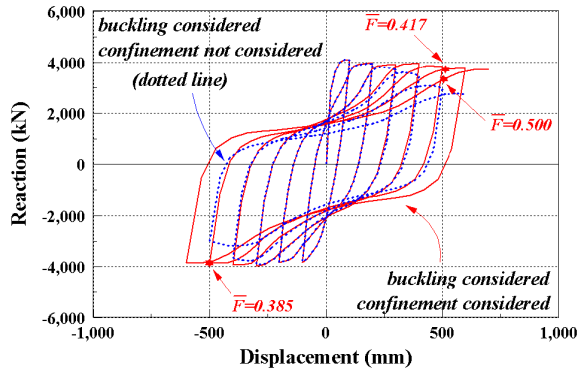


Fig.10.2 Confinement effect on response and damage index of large-scale section

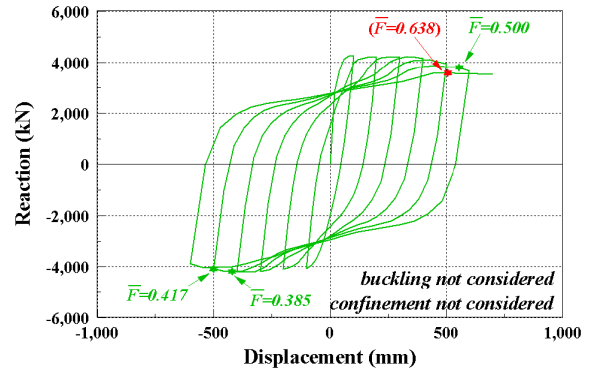


Fig.11.2 Buckling effect on response and damage index of large-scale section

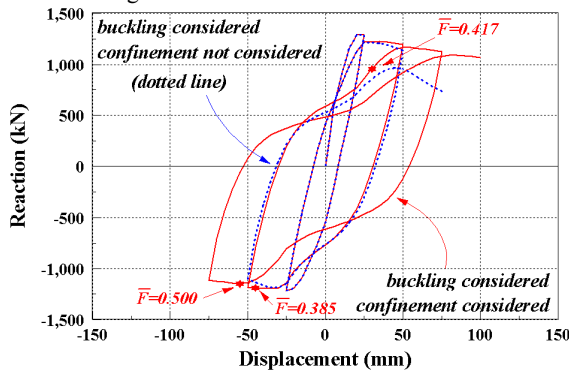


Fig.10.3 Confinement effect on response and damage index of medium-scale section under high compression

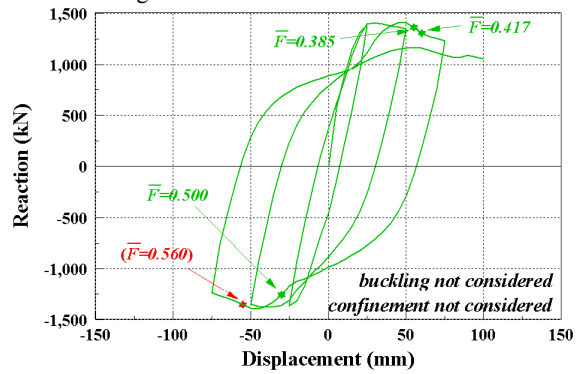


Fig.11.3 Buckling effect on response and damage index of medium-scale section under high compression

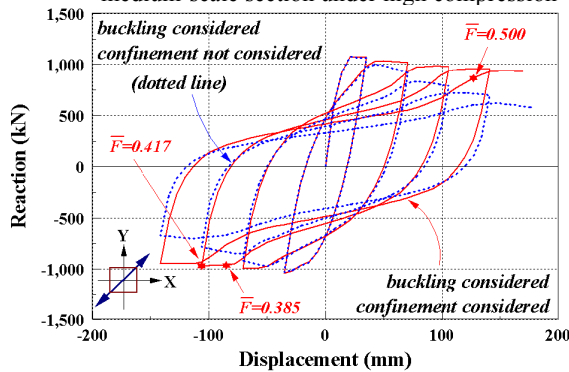


Fig.10.4 Confinement effect on response and damage index of medium-scale section under skew loading (45 degree)

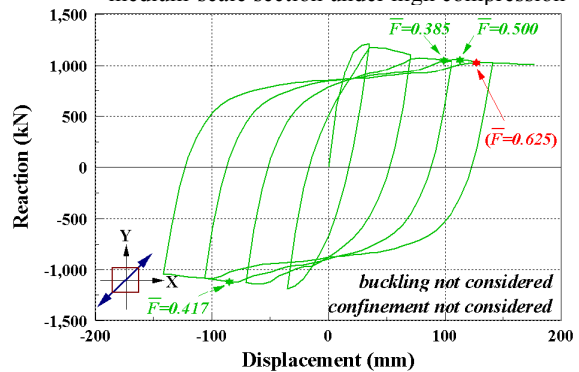


Fig.11.4 Buckling effect on response and damage index of medium-scale section under skew loading (45 degree)

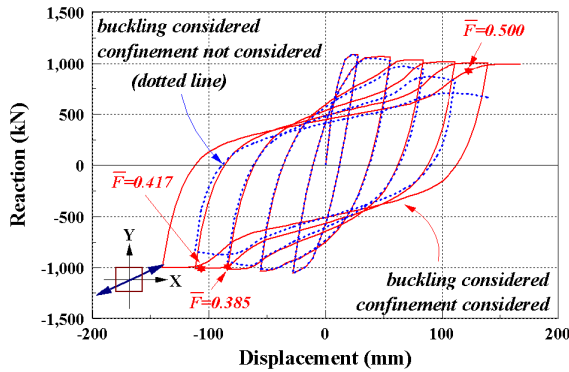


Fig.10.5 Confinement effect on response and damage index of medium-scale section under skew loading (22.5 degree)

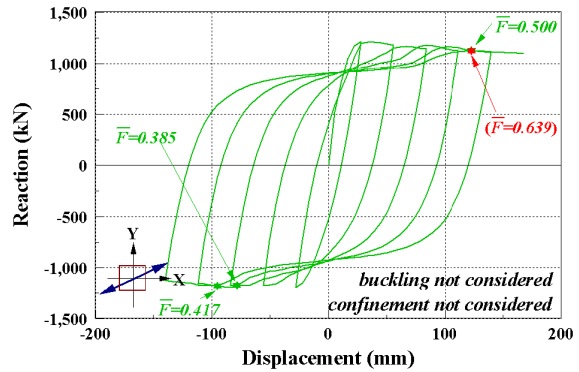


Fig.11.5 Buckling effect on response and damage index of medium-scale section under skew loading (22.5 degree)

It can be clearly seen in **Figs. 10.1 to 10.5** that member flexural ductility is improved by restraining the evolution of fractures as the strain rises by providing confinement. Simultaneously, the increase of the cross section damage index is also restrained. In this case, it is found that the response displacement point at which the horizontal load decreases from the peak capacity somewhat coincides with the cross-sectional damage index of 0.500. Thus in carrying out response analysis of column members in which flexural ductility is improved by confinement, the proposed damage index may have general applicability to the assessment of seismic performance Level 2. Although details of the fracture evolution law at each point over the cross section, as determined by the arrangement of lateral ties, can be calculated using three-dimensional nonlinear analysis up to peak capacity, the authors will wait for future research into compressive softening behavior under confinement stress, for example, for applicability beyond the peak [14][15].

## **6. PAPAMETRIC ANALYSIS AND INVESTIGATION OF SAFETY MARGIN**

### **6.1 Investigation of Static Loading**

The analytical investigation described so far considers buckling of the main reinforcement [8]. Generally, as concrete comes under increasing bending compression, deformation progresses and the concrete damage level increases once the compression-resisting mechanism of the main reinforcement is lost. While neglecting the confinement effect in a performance evaluation results in results that err on the safe side, neglecting the buckling of reinforcing bars causes an error on the side of danger. Therefore, if buckling behavior is to be neglected in the nonlinear response analysis of deformation and damage, it is necessary to define a safety factor of greater than 1.0.

**Figures 11.1 to 11.5** indicate member response behavior under static one-axis loading and the cross-sectional damage index for the case where buckling and swelling-out in the transverse direction are neglected. The confinement effect of concrete is not taken into account. Comparing the results given in **Figs. 10** and **Figs. 11** leads to the following considerations.

Looking first at the envelope of the load-displacement relationship, the response curves are found to be similar in two groups of cases in which the compressive reaction of the reinforcement is fully considered: one where confinement effect and buckling behavior are neglected, and the other where both phenomena are taken into account. Within the range investigated in this research, this tendency is observed regardless of cross-sectional dimensions and loading method. The influence of reinforcement buckling is relatively smaller with larger structures and smaller-diameter reinforcing bars. On the other hand, it is recognized that confinement effect and buckling behavior, when neglected, apparently negate each other on the envelope curve for target columns with structural dimensions based on designs in actual use.

In **Figs. 11.1 to 11.5**, values of damage index  $\bar{F}$  range from 0.560 to 0.639 in simulations where confinement effect and buckling behavior are ignored, while values reach 0.500, the value thought to coincide with ultimate displacement, in simulations where both are considered. This means that a completely safe evaluation can be obtained for members under static reversed cyclic loading if structural analysis factor  $\gamma_a$  is made 1.1 times greater when confinement effect and buckling behavior are neglected as when they are fully accounted for. However, simulations in which these phenomena are neglected indicate superior energy absorption in the internal loop in the load-displacement diagram while it is small in simulations considering them. Further, when dynamic loading is assumed, the influence of neglecting them may be large, especially in the case of ductile columns, and it is thought necessary to determine a structural analysis factor that adjusts for this.

### **6.2 Investigation of Dynamic Loading**

The investigation described so far deals mainly with one-axis static loading. If the influence of confinement effect and main reinforcement buckling are to be taken into account in the structural analysis factor, it is necessary to investigate not only static loading based on forced displacement but also dynamic loading, since there are differences in the internal loop in the load-displacement diagram.

The current performance verification method generally allows for independent judgment of dynamic response behavior under design ground motion in the two horizontal orthogonal directions [3]. The

investigation here is also limited to one horizontal direction, as following suit. Addition to the aforementioned medium-scale RC column, RC column road bridge pier subjected to eccentric axial force is selected as the target structure. It is known that RC columns subjected to eccentric axial force exhibit a multi-axis response even if loading is in one direction only [4], and this situation is suitable for the application of dynamic nonlinear response analysis based on material mechanical models.

Three different artificial seismic waveforms, as shown in Figs. 12, 14, and 16, are applied to the base of the medium-scale RC column, and the forced vibrations are simulated. The phase characteristics of the waveform in Fig. 16 are quoted from the literature [18][19]. The time history of response displacement and restoring force characteristics are given as analytical results in Figs. 13, 15, and 17. In this dynamic analysis, direct integration based on Newmark's  $\beta$  method ( $\beta = 0.36$ ) is carried out and viscous damping is not considered.

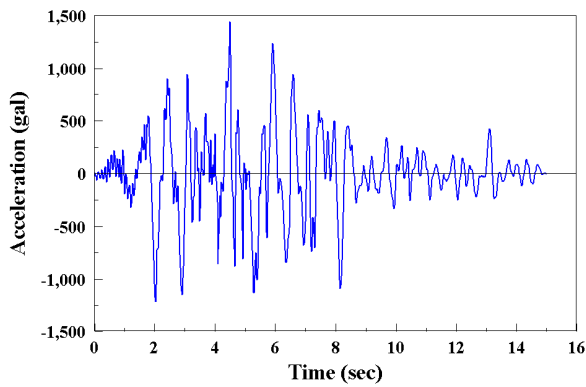


Fig.12 Horizontal one-axis input motion 1

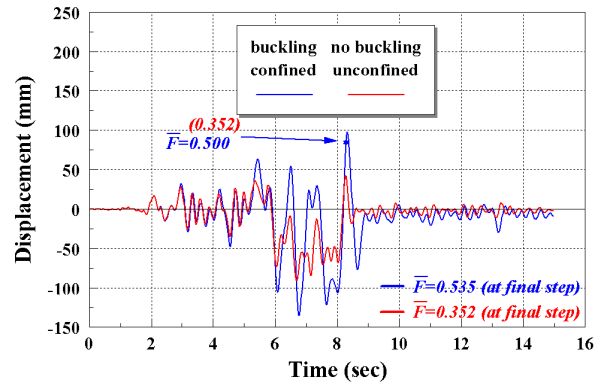


Fig.13.1 Time history of response displacement under input motion 1

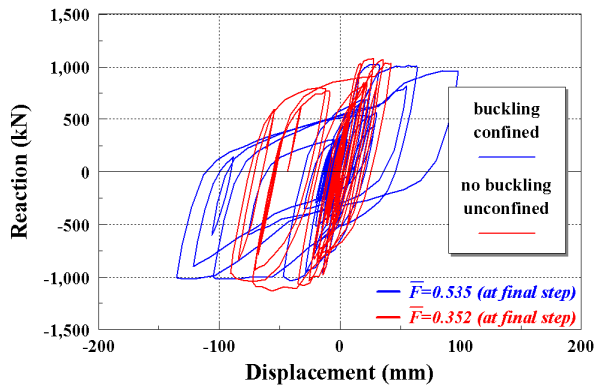


Fig.13.2 Restoring force characteristic under input motion 1

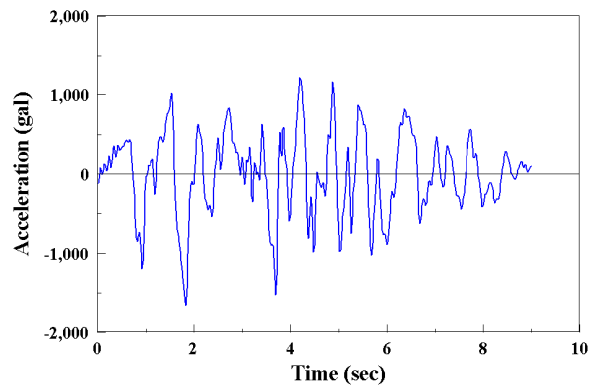


Fig.14 Horizontal one-axis input motion 2

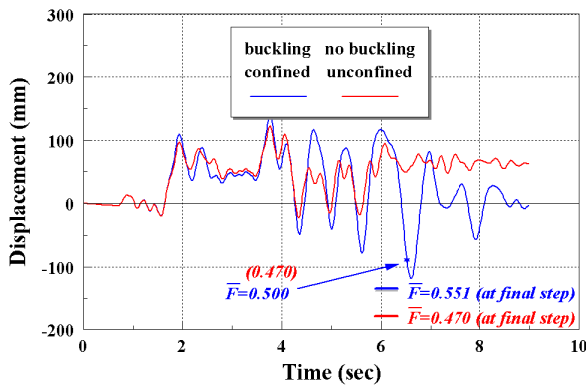


Fig.15.1 Time history of response displacement under input motion 2

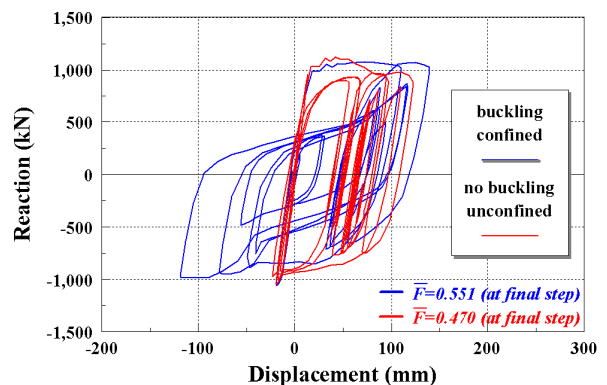


Fig.15.2 Restoring force characteristic under input motion 2

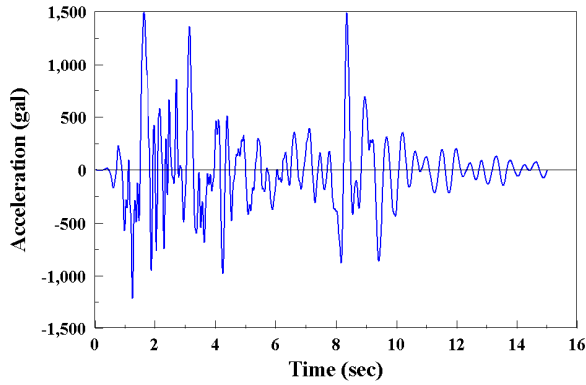


Fig.16 Horizontal one-axis input motion 3 [18][19]

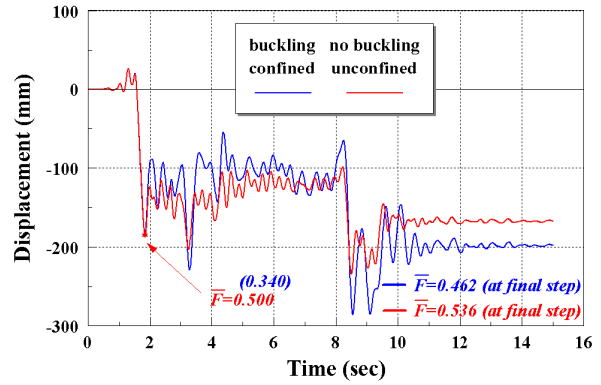


Fig.17.1 Time history of response displacement under input motion 3

The results of this analysis show that response displacement when confinement effect and buckling behavior are taken into account is larger than when they are neglected, since stiffness and energy absorption are both lower. Generally, damage index  $\bar{F}$  tends to be large in simulations where the confinement effect and buckling behavior are considered, as in Figs. 13 and 15. In these examples, the value of the damage index is 0.352 and 0.470 in the simulations neglecting confinement effect and buckling behavior, while it reaches 0.500 in the simulation considering both. However, this tendency is reversed in some cases, depending on the seismic waveform and on structural dimensions; see Fig. 17.

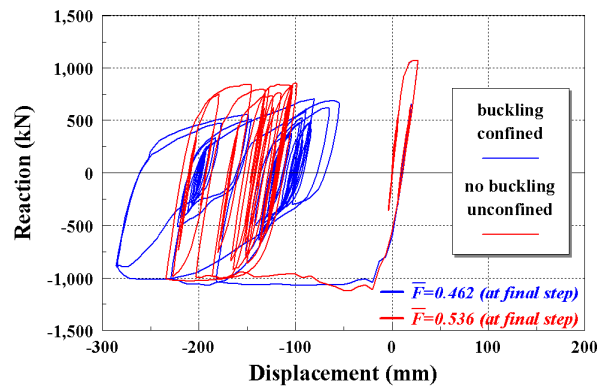


Fig.17.2 Restoring force characteristic under input motion 3

Next, seismic motion is applied to the base of an RC column under eccentric axial loading [4][20] in the 45 degree direction to the moment derived from the eccentric axial force, as shown in Fig. 18.1, and forced vibration is simulated. The average axial compressive stress is set at  $0.56 \text{ [N/mm}^2\text{]}$ , and the artificial waveform is that shown in Fig. 7.2 but with the amplitude multiplied by 1.2 times. From the analytical results in Figs. 18.2 to 18.6, RC column responses are seen to arise in multiple axes due to the complex effect of the inertial force and moment resulting from the fixed eccentric axial force. In this example, both response displacement and damage index are larger in the simulation where confinement effect and buckling behavior are ignored. Differences in degree of capacity degradation after the yield point give rise to differences in response displacement, and neglecting the confinement effect and buckling behavior results in evaluations on the safe side.

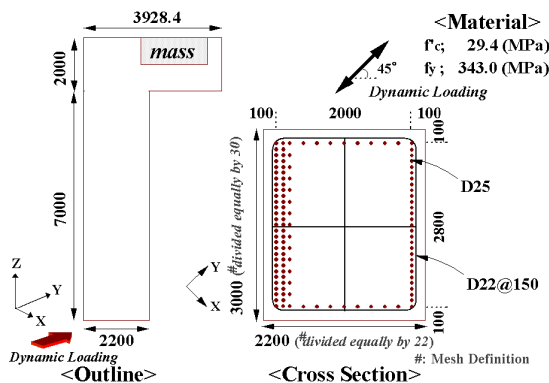


Fig.18.1 Structural dimensions of eccentric axial force column

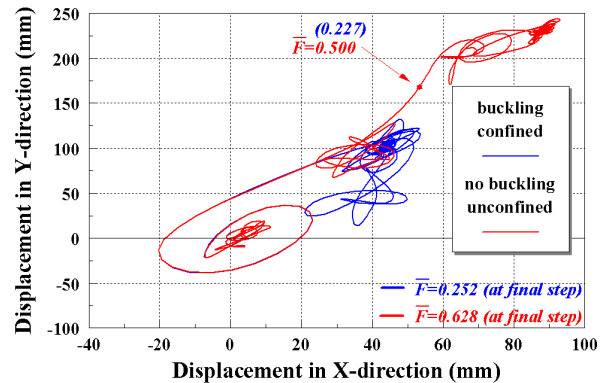


Fig.18.2 Horizontal response displacement

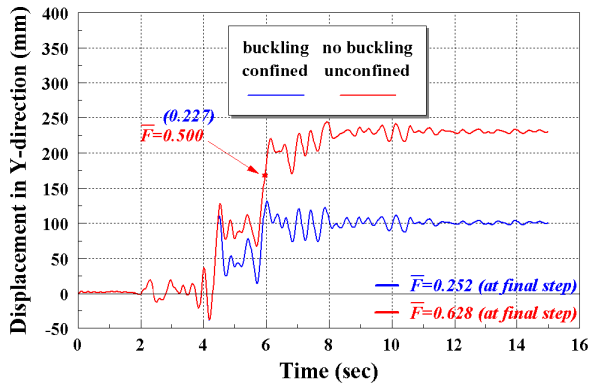


Fig.18.3 Time history of response displacement in Y-direction

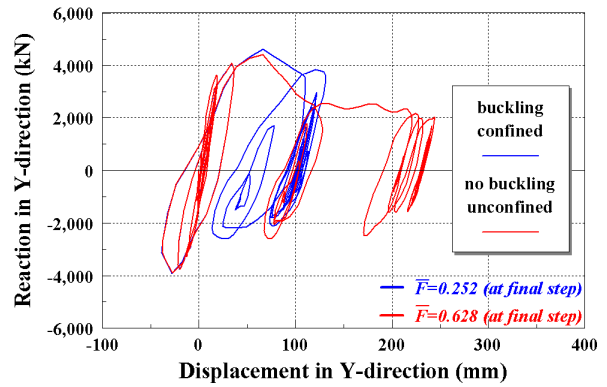


Fig.18.4 Restoring force characteristic in Y-direction

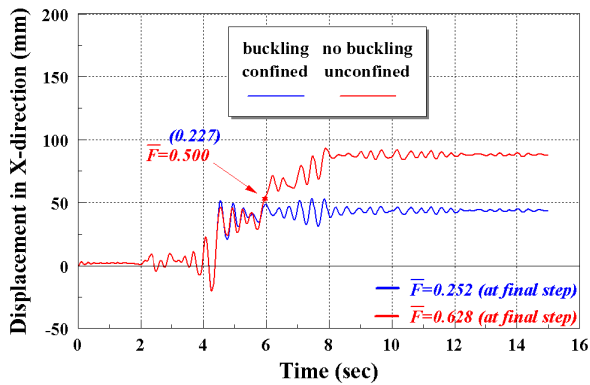


Fig.18.5 Time history of response displacement in X-direction

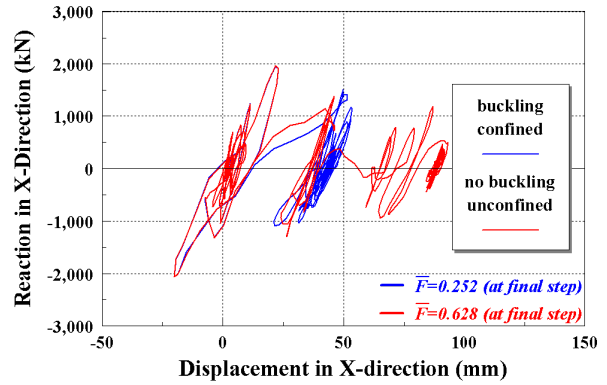


Fig.18.6 Restoring force characteristic in X-direction

Further, member response and damage when subjected to seismic motion in two horizontal orthogonal and the vertical direction are investigated, with a view to the future direction. Artificial seismic waveforms with three orthogonal components are applied to the base of a medium-scale RC column, and the forced vibrations are simulated. The artificial motion shown in Fig. 7.2 is used, with the amplitude multiplied by 1.08 times. The analytical results are shown in Figs. 19.1 to 19.5. RC column responses beyond yield displacement complicatedly in the multi-direction in this analysis, and difference between the simulation considering and neglecting confinement effect and buckling behavior is very large. This suggests that when determining the structural analysis factor for members with high ductility, a larger margin should be applied if confinement effect and buckling behavior are neglected.

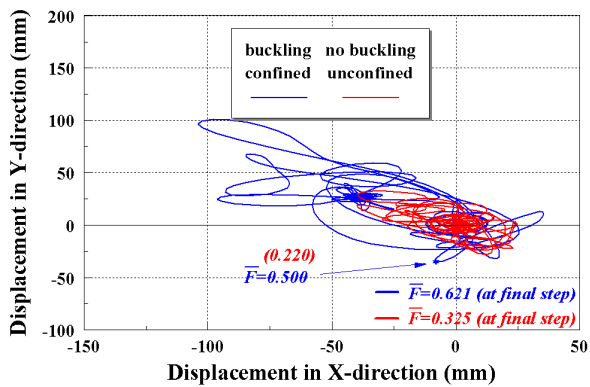


Fig.19.1 Horizontal response displacement under multi-axis motion

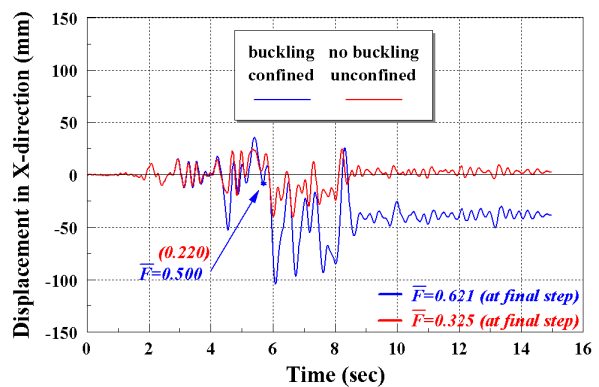


Fig.19.2 Time history of response displacement in X-direction

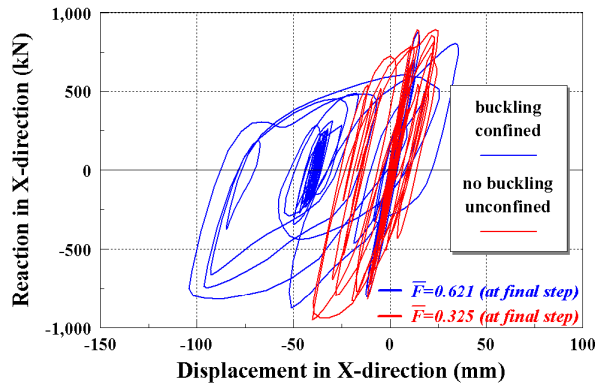


Fig.19.3 Restoring force characteristic in X-direction

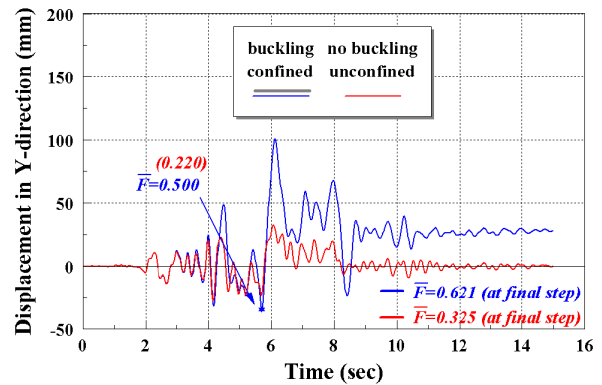


Fig.19.4 Time history of response displacement in Y-direction in time history

Because the natural period of structures increases after yield, the response behavior under dynamic loading is strongly affected by the phase characteristics of the ground motion. It is also well known that response characteristics have no simple relationship to the use or otherwise of a confinement or buckling model and to variations in material properties. And, although forced vibration without restraint was allowed for column members in this study, actual structures and members are restrained somewhat due to indeterminate order or adjacent structural members, etc. To take this in account when investigating seismic safety, the influence of ground motion, especially its phase properties, including the effect of multi-axis input on various structure types with arbitrary geometry or material strength, must be considered. This is an issue that requires further study

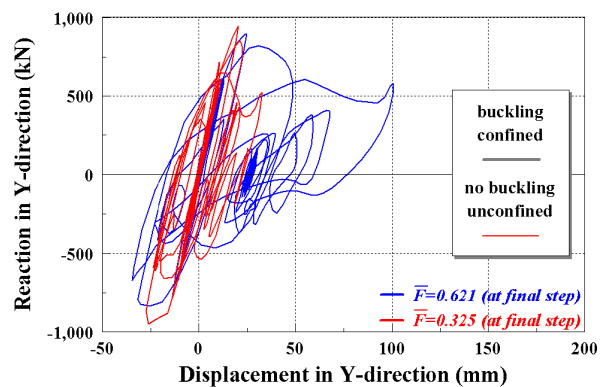


Fig.19.5 Restoring force characteristic in Y-direction

## 7. CONCLUSIONS

The conclusions drawn from this work are as follows:

- 1) The level of damage to RC beam-column members can be easily determined using the proposed damage index, which is the sectional averaged value of the concrete fracture parameter as calculated from the elasto-plastic fracture model.
- 2) For RC columns representative of actual pier dimensions used for road and railway bridges in Japan, the limit value of cross-sectional damage index for seismic performance Level 2 may be given as 0.500. This is thought to be approximately equivalent to the limit state for seismic performance Level 2 as defined in member mechanical models from the view of concrete damage.
- 3) The confinement effect can be taken into account simply by altering the parameter defining fracture evolution, and the limit value stated in 2) above applies even when member ductility is improved due to the confinement effect.
- 4) The proposed damage index is generally applicable, such as to multi-axis dynamic loading, varying axial force, and loading on an eccentric axis, etc.

Equations (1) to (3) in this paper are applicable on condition that the element length in the region of the maximum moment is set at 200 [mm]. If a different element length is defined, the relationship between

concrete stress and strain in the softening range must be modified based on the energy equilibrium. At this moment, use of the strain value in the cross section as a damage index is not appropriate because the response strain value is strongly affected by the mesh definition. It is also difficult to use the stress value as an evaluation of seismic performance in the softening range, because two corresponding strain values exist for a particular stress value. On the other hand, the proposed cross-sectional damage index offers the advantage of being independent of softening properties in the material model because the relationship between fracture parameter and maximum experienced strain is formulated according to element length.

The discussion in this paper is limited to normal-strength concrete. It is well known that softening behavior after the peak is different in high-strength concrete and steel-fiber concrete than in normal-strength concrete. The fracture evolution law for such concretes is gradually coming into qualitative focus, so we wait expectantly to assess the applicability of this damage index to other kinds of concrete to future research.

### Acknowledgements

The authors would like to express their gratitude to Professor Hiroshi SHIMA of Kochi University of Technology, Japan, for the invaluable advice received during the course of this study.

### References

- [1] Harada, M., Onitsuka, S., Adachi, M., and Matsuo, T., "Experimental Study on Deformation Performance of Cylindrical Reinforced Concrete Structure", *Proc. of JCI*, Vol.23, No.3, pp.1129-1134, July 2001. (in Japanese)
- [2] JSCE, "Standard Specification for Design and Construction of Concrete Structure, Seismic Design", 1996.
- [3] Tsuchiya, S., Ogasawara, M., Tsuno, K., Ichikawa, H., and Maekawa, K., "Multi-Directional Flexure Behavior and Nonlinear Analysis of RC Columns Subjected to Eccentric Axial Forces", *Concrete Library International*, No.37, pp.1-15, JSCE, June 2001.
- [4] Maekawa, K. and Okamura, H., "The Deformational Behavior and Constitutive Equation of Concrete Using the Elasto-Plastic Fracture Model", *Journal of the Faculty of Engineering, the University of Tokyo (B)*, Vol.37, No.2, pp.253-328, 1983.
- [5] Kato, B., "Mechanical Properties of Steel under Load Cycles Idealizing Seismic Action", *CEB Bulletin D'Information*, No.131, pp.7-27, 1979.
- [6] CEB, "RC Elements under Cyclic Loading –State of the Art Report", *Thomas Telford*, 1996.
- [7] Dhakal, R. and Maekawa, K., "Post-Peak Cyclic Response Analysis and Energy Dissipation Capacity of RC Columns", *Proc. of JSCE*, No.676/V-51, pp.117-133, May 2001.
- [8] Dhakal, R. and Maekawa, K., "Post-Peak Cyclic Behavior and Ductility of Reinforced Concrete Columns", *Modeling of Inelastic Behavior of RC Structures under Seismic Loads*, edited by Tanabe, T. and Benson, S., ASCE, pp.193-216, 2001.
- [9] Maekawa, K., Takemura, J., Irawan, P., and Irie, M., "Continuum Fracture in Concrete Nonlinearity under Triaxial Confinement", *Proc. of JSCE*, No.460/V-18, pp.113-122, February 1993.
- [10] Watanabe, T., Tanimura, Y., Takiguchi, M., and Sato, T., "Evaluation Method of Deformation Capacity Related to Damage Conditions for Reinforced Concrete Members", *Proc. of JSCE*, No.683/V-52, pp.31~45, August 2001. (in Japanese)
- [11] Hoshikuma, J., Unjo, S., and Nagaya, K., "Size Effect on Inelastic Behavior of Reinforced Concrete Columns Subjected to Cyclic Loading", *Proc. of JSCE*, No.669/V-50, pp.215~232, February 2001. (in Japanese)
- [12] Amano, R., "Development of New Construction Method in Concrete Structures", *Ph. D. Dissertation of University of Tokyo*, 1999. (in Japanese)
- [13] Torsak, L., Watanabe, K., Matsuo, M., and Niwa, J., "Experimental Study on Parameters in Localization of Concrete Subjected to Compression", *Proc. of JSCE*, No.669/V-50, pp.309~321, February 2001.
- [14] Nakamura, H. and Higai, T., "Compressive Fracture Energy and Fracture Zone Length of Concrete", *Modeling of Inelastic Behavior of RC Structures under Seismic Loads*, edited by Tanabe, T. and Benson, S., ASCE, pp.471-487, 2001.
- [15] Pallewatta, T. M., Irawan, P., and Maekawa, K., "Effectiveness of Laterally Arranged Reinforcement on the Confinement of Core Concrete", *Proc. of JSCE*, No.520/V-28, pp.297-308, August 1995.

- [16] Pallewatta, T. M., Irawan, P., and Maekawa, K., "Verification of 3D Constitutive Models of Concrete in Line with Capacity and Ductility of Laterally Reinforced Concrete Columns", *Proc. of JSCE*, No.520/V-28, pp.309-321, August 1995.
- [17] RTRI, "Railway Structures Standard Specification for Design, Seismic Design", Maruzen, October 1999. (in Japanese)
- [18] JSCE, "Design and Construction Guideline Draft for Self-Compacting High Strength and High Durable Concrete Structures –An attempt to Structures of New Generation Transportation System–", *Concrete Library 105*, June 2001. (in Japanese)
- [19] Kosaka, H., Ogasawara, M., Tsuno, K., Ichikawa, H., and Fukuda, A., "Seismic Performance Verification Experiment of RC Piers Subjected to Torque", *Proc. of the First Symposium on Seismic Design Based on Capacity Design*, pp.167-170, January 1998 (in Japanese)